Article

Volume 14, Issue 2, 2025, 70

https://doi.org/10.33263/LIANBS142.070

Arcangelisia flava as a SARS-CoV-2 M^{Pro} Inhibitor: Molecular Docking, ADME Studies, and Toxicity Prediction

Mohammad Rizki Fadhil Pratama ^{1,2,*}, Suratno Suratno ^{1,3}, Evi Mulyani ¹, Aso Hameed Hasan ⁴, Ahmed Mahal ⁵, Tohfa Aslan Nasibova ⁶, Lina O. Perekhoda ⁷, Broto Santoso ⁸, Hadi Poerwono ⁹, Siswandono Siswodihardjo ⁹

- Department of Pharmacy, Universitas Muhammadiyah Palangkaraya, Palangka Raya, Central Kalimantan, Indonesia; mohammadrizkifadhilpratama@umpr.ac.id (M.R.F.P.); nono.suratno89@yahoo.com (S.S.); evi.muly4ni@gmail.com (E.M.);
- Doctoral Program of Pharmaceutical Science, Faculty of Pharmacy, Universitas Airlangga, Surabaya, East Java, Indonesia; mohammadrizkifadhilpratama@umpr.ac.id;
- Doctoral Program of Pharmaceutical Science, School of PhD Studies, Semmelweis University, Üllői u. 26, Budapest, Hungary; nono.suratno89@yahoo.com;
- Department of Chemistry, College of Science, University of Garmian, Bardesur Street, Kalar, Kurdistan Region, Iraq; aso.hameed@garmian.edu.krd;
- Department of Medical Biochemical Analysis, College of Health Technology, Cihan University-Erbil, Erbil, Kurdistan Region, Iraq; ahmed.mahal@cihanuniversity.edu.iq;
- 6 Department of General and Toxicological Chemistry, Azerbaijan Medical University, Baku, Azerbaijan; drtohfe@gmail.com;
- Department of Pharmaceutical Chemistry, National University of Pharmacy, Hryhoriia Skovorody St, Kharkiv, Kharkiv Oblast, Ukraine; lina_perekhoda@nuph.edu.ua;
- Department of Pharmaceutical Chemistry, Faculty of Pharmacy, Universitas Muhammadiyah Surakarta, Surakarta, Central Java, Indonesia; broto.santoso@ums.ac.id;
- Department of Pharmaceutical Science, Faculty of Pharmacy, Universitas Airlangga, Surabaya, East Java, Indonesia; hadip@ff.unair.ac.id (H.P.); prof.sis@ff.unair.ac.id (S.S.)
- * Correspondence: mohammadrizkifadhilpratama@umpr.ac.id;

Scopus Author ID 56925239400A

Received: 3.04.2024; Accepted: 30.06.2024; Published: 15.02.2025

Abstract: This study aims to identify active compounds of *Arcangelisia flava*, which can potentially inhibit SARS-CoV-2 M^{Pro}, through *in silico* studies. Molecular docking was carried out on 11 primary known metabolites of *A. flava* against the SARS-CoV-2 M^{Pro} receptor with remdesivir as a reference compound. All the ligands were analyzed for their ADME profile using a combination of SwissADME and pkCSM. The toxicity profile of each ligand was then predicted by ProTox-II. The best docking results were shown by 6-hydroxyfibraurin with a difference in the free energy of binding 0.48 kcal/mol higher than remdesivir, while the highest similarity interaction with remdesivir was shown by berberine with 52.27%. All ligands showed relatively similar ADME profiles and acceptable drug-likeness properties, including toxicity. In conclusion, 6-hydroxyfibraurin has the potential as a SARS-CoV-2 M^{Pro} inhibitor with acceptable ADME and toxicity profiles. Further *in vitro* and *in vivo* studies are needed to prove the compound's activity.

Keywords: 6-hydroxyfibraurin; *Arcangelisia flava*; Covid-19; molecular docking; SARS-CoV-2 M^{Pro}.

© 2025 by the authors. This article is an open-access article distributed under the terms and conditions of the Creative Commons Attribution (CC BY) license (https://creativecommons.org/licenses/by/4.0/).

1. Introduction

After peaking in the first trimester of 2021 [1], cases of coronavirus disease 2019 (COVID-19) began to show signs of being under control in the final trimester of 2021 [2]. In addition to the ever-expanding global vaccination coverage [3], understanding the coronavirus that causes severe acute respiratory syndrome 2 (SARS-CoV-2) is another important component [4]. After the SARS-CoV-2 delta variant outbreak, which took many lives worldwide, especially in developing countries such as India and Indonesia [5], there were signs of a decline in the rate of cases and death rates worldwide. Nevertheless, there is always the possibility of the emergence of novel, more vicious variants in the future, and the world must be prepared to deal with it. One is developing complementary therapies to support vaccination campaigns, currently the first line of action in handling the COVID-19 pandemic [6].

The development of oral therapy for COVID-19 is the main focus of many researchers from various countries because it can complement the limitations of vaccination in distribution and administration [7]. Several therapeutic targets have been identified, and apart from spike protein and RNA-dependent RNA polymerase (RdRp) [8], the main protease of SARS-CoV-2 (SARS-CoV-2 M^{Pro}) is one of the most attractive targets in the development of the COVID-19 therapy [9,10]. The repurposing of several available drugs has been reported to interact with the enzyme and inhibit the replication and transcription process of SARS-CoV-2, including remdesivir, the reference compound for developing inhibitors for this target [11]. Moreover, after reporting on the potential of repurposing drugs [12] and novel drug compounds [13-15] as SARS-CoV-2 M^{Pro} inhibitors, the researchers turned their attention to one of the oldest sources of medication on earth: metabolites from medicinal plants [16].

The exploration of SARS-CoV-2 M^{Pro} inhibitors derived from natural ingredients is still a fascinating topic. However, several medicinal plants have been reported for their activity [17], including *Curcuma longa* [18], *Andrographis paniculata* [19], *Nigella sativa* [20], *Glycyrrhiza glabra* [21], *Withania somnifera* [22], *Artemisia annua* [23], *Camellia sinensis* [24], and *Garcinia mangostana* [25]. However, these plants have yet to be officially used in the therapy of COVID-19, even though they have been shown *in silico* and *in vitro* activities, except as complementary therapy [26]. Naturally, these circumstances encourage scientists to investigate medicinal plants with the greatest potential for acting as M^{Pro} inhibitors of SARS-CoV-2. Furthermore, after the activities of various medicinal plants were investigated and reported by researchers around the world, it turns out that there is one medicinal plant from Indonesia whose potential as a SARS-CoV-2 M^{Pro} inhibitor has never been studied: *Arcangelisia flava*.

Arcangelisia flava or yellow root (Indonesian: 'akar kuning') is a medicinal plant from Indonesia known to have various biocidal activities such as antimicrobial [27] and antifungal [28]. The stems contain various alkaloids, such as berberine [29], and diterpenoids, such as fibraurin [30], with broad activity potential. However, no studies have reported the potential of various metabolites of *A. flava* as SARS-CoV-2 M^{Pro} inhibitors. Thus, this study aims to determine which *A. flava* active substance can most suppress SARS-CoV-2 M^{Pro}. Several web servers were used to determine the properties of these metabolites in terms of absorption, distribution, metabolism, excretion, and toxicity (ADMET) after the molecular docking method was applied in an *in silico* manner. In the final step, predictions of the toxicity of these metabolites were carried out to determine the probability of toxic properties and predicted LD₅₀ of each metabolite.

2. Materials and Methods

2.1. Hardware and software.

The hardware and software (including three web servers: SwissADME, pkCSM, and ProTox-II) used in this study were the same as those used in our previous study [31].

2.2. Ligands preparation.

Eleven known secondary metabolites were reported in the roots of *A. flava* used as test ligands [27,32], while the reference ligand was remdesivir [33], as shown in Table 1. The stages of the ligand preparation process were carried out in the same way as in our previous study [31].

Table 1. The two-dimensional structure of all test and reference ligands.

Code Ref	Name	Two-dimensional structure
	Remdesivir	H ₂ N N N N N N N N N N N N N N N N N N N
1	2-dehydroaxyarcangelisinol	OH OH
2	6-hydroxyarcangelisin	OH OH
3	6-hydroxyfibleucin	OH OH
4	6-hydroxyfibraurin	OH OH

Code	Name	Two-dimensional structure
5	Berberine	
6	Columbamine	HO
7	Fibleucin	OH H
8	Fibraurin	
9	Jatrorrhizine	HO No
10	Palmatine	N. O.
11	Tinophyllol	HO

2.3. Receptor preparation.

The receptors used was SARS-CoV-2 M^{Pro} (PDB ID 6LU7) from Protein Data Bank's website with a co-crystal ligand of N-[(5-methylisoxazol-3-yl)carbonyl]alanyl-l-valyl-N~1~-

((1R,2Z)-4-(benzyloxy)-4-oxo-1-{[(3R)-2-oxopyrrolidin-3-yl]methyl}but-2-enyl)-leucinamide [9]. The receptor contains the single chain of the main protease monomer from SARS-CoV-2 with a resolution of 2.16 Å.

2.4. Molecular docking.

The docking protocol validation was carried out using the redocking method reported by our previous study using the same receptor [14], with the same stages as our previous study [31]. The observed parameter was a root-mean-square deviation (RMSD), which was not more than 2 Å. The docking procedure was conducted five times, and the average and deviation values were used to compute the free energy of binding (ΔG ; kcal/mol) value that was obtained [34].

The grid box sizes and locations at the receptor were identical for all test and reference ligands, and docking was carried out in the same manner as validation. The gathered data was categorized into two parameters: ΔG and ligand-receptor interactions. The latter was determined by calculating the average similarity percentage between the interactions and the interactions between the interacting amino acids. Similar to the validation procedure, there were five iterations of the docking process. Each test ligand's two properties were compared to remdesivir to see if they were similar, and then the results were created in a two-dimensional graph, as shown in our earlier study [35].

2.5. ADMET prediction.

The ADMET properties of each test ligand were predicted by using the procedures described in our earlier study [36], which used multiple ADMET prediction web servers to produce thorough results. OpenBabel 3.1.1 was used to convert each test ligand into its standard SMILES format. The ADMET property prediction findings were then presented graphically, as demonstrated by Sukardiman *et al.* [37].

3. Results and Discussion

3.1. Molecular docking.

The redocking procedure yielded an RMSD value of 1.981 Å for the 6LU7 receptor. This demonstrated that the receptor's docking procedure was appropriate for docking. Figure 1 shows the visual representation of ligand overlays from redocking with co-crystal ligands from crystallographic data.

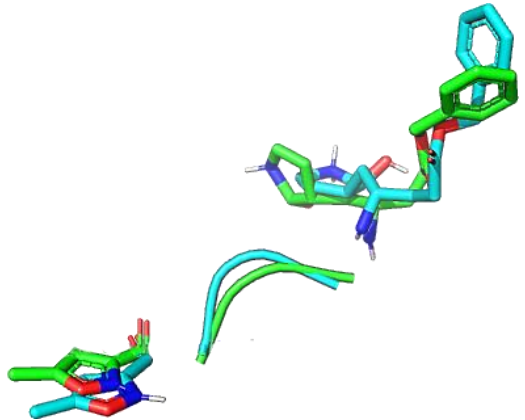


Figure 1. Overlays of redocking ligands (blue) with co-crystal ligands from X-crystallography data (green) at receptors 6LU7 with RMSD 1.981 Å.

Twenty-five amino acids interact at the 6LU7 receptor, nine forming hydrogen bonds. Table 2 displays the metrics that were noticed during the validation process, which include amino acid interactions and ΔG , in addition to the grid box's size and coordinates. This result is similar to our previous report because the protocol used is the same [34] except for the exhaustiveness and number of modes, which were increased to 128 and 20, respectively, to improve the accuracy of docking results [38].

Table 2. Results of the validation process.

Parameters	Value
PDB ID	6LU7
Co-crystal	$N-[(5-\text{methylisoxazol-}3-\text{yl})\text{carbonyl}]$ alanyl-l-valyl- $N\sim 1\sim -((1R,2Z)-4-(\text{benzyloxy})-4-\text{oxo-}1-\{[(3R)-2-(1R,2Z)-4-(\text{benzyloxy})-4-\text{oxo-}1-((1R,2Z)-4-(\text{benzyloxy})-4-\text{oxo-}1-((1R,2Z)-4-(\text{benzyloxy})-4-\text{oxo-}1-((1R,2Z)-4-(\text{benzyloxy})-4-\text{oxo-}1-((1R,2Z)-4-(\text{benzyloxy})-4-\text{oxo-}1-((1R,2Z)-4-(\text{benzyloxy})-4-\text{oxo-}1-((1R,2Z)-4-(\text{benzyloxy})-$
ligand	oxopyrrolidin-3-yl]methyl}but-2-enyl)-l-leucinamide
Grid box size	40 x 54 x 40
(Å)	
Grid box	x: -9.732
position	y: 11.403
	z: 68.483
RMSD (Å)	1.981
ΔG (kcal/mol)	-8.12 ± 0.04
Amino acid	24-Thr ^a
residues	25-Thr ^a
	26-Thr ^a
	41-His ^b
	49-Met ^b
	54-Tyr ^a
	140-Phe ^c
	141-Leu ^d
	142-Asn ^a
	143-Gly ^c
	144-Ser ^a
	145-Cys ^a
	163-His ^c 164-His ^c
	165-Met ^c
	166-Glu ^c
	167-Leu ^b
	168-Pro ^b
	172-His ^c
	187-Asp ^a
	188-Arg ^a
	189-Gln ^c
	190-Thr ^c
	191-Ala ^b
	192-Gln ^a
9 7 7 1	172-0m

^a Van der Waals interaction; ^b Alkyl/Pi-alkyl interaction; ^c Hydrogen bond; ^d Pi-Pi T-shaped/Pi-Pi Stacked/Amide-Pi stacked.

Berberine, one of the primary metabolites of *A. flava*, known to have various activities, was not the ligand with the best docking results. The ΔG value of berberine was -7.14±0.05 kcal/mol, while remdesivir was -8.38±0.08 kcal/mol or a difference of 1.24 kcal/mol. Meanwhile, the ligand with the closest ΔG value to remdesivir was 6-hydroxyfibraurin with -7.9±0 kcal/mol, or only 0.48 kcal/mol difference. 6-hydroxyfibraurin also revealed a moderate similarity of the ligand-receptor interaction to remdesivir at 50% or half of the interaction. This value is slightly lower than berberine as a ligand, with the highest similarity of 52.27%. Uniquely, the four ligands (6-hydroxyarcangelisin, fibraurin, 6-hydroxyfibleucin, and palmatine) had 0% similarity, indicating that they interact on the different binding sites with remdesivir. Palmatine also showed the most considerable ΔG difference to remdesivir with 2.04 kcal/mol, making it the less favorable ligand at the binding site. For easier-to-understand

observation, the values of these two parameters for every ligand were then shown on a twodimensional graph, as presented in Figure 2.

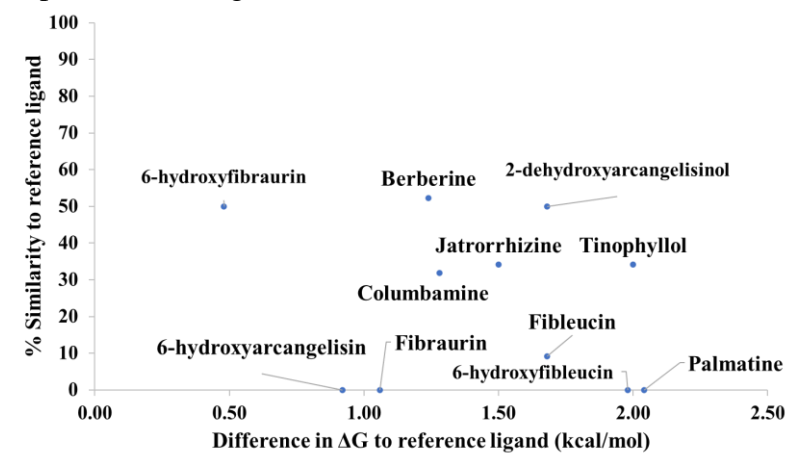


Figure 2. The two-dimensional graph between the difference in the value of ΔG and the % similarity of ligand-receptor interactions compared to reference ligand.

3.2. ADMET prediction.

Five criteria were used to categorize the three web servers' predictions of ADMET properties: toxicity, distribution, metabolism, excretion, and absorption. In Figure 3, absorption parameters were acquired from prediction utilizing SwissADME and pkCSM to various factors, such as water solubility, ESOL Log S, Ali Log S, MLOGP, XLOGP3, MLOGP, Silicos-IT Log P, consensus Log P, and implicit Log P (iLOGP). The findings demonstrate that compound 9 (jatrorrhizine) had the highest water solubility compared to the other ligands, whereas compound 4 (6-hydroxyfibraurin) had the lowest water solubility.

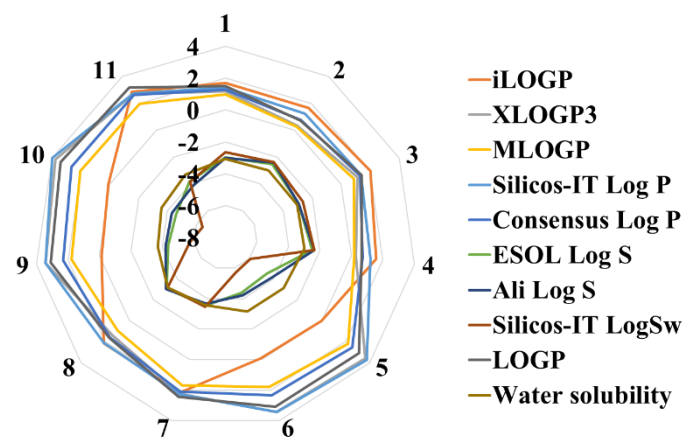


Figure 3. Prediction of test ligand absorption parameters with SwissADME and pkCSM. The highest and lowest water solubility prediction was shown by compounds 9 and 4, respectively.

As shown in Figure 4, the results obtained with pkCSM for distribution parameters reveal fluctuations in numerous parameters, including % unbound, blood-brain barrier (BBB) permeability, central nervous system (CNS) permeability, and volume of distribution at steady-state (VDss). Most of the ligands (7 out of 11) showed negative BBB permeability values, and all of them showed negative CNS permeability values, indicating that the distribution of the ligands in the BBB and CNS tissues was relatively high. The ligand with the lowest BBB permeability value was compound 8 (fibraurin), while the lowest CNS permeability value was compound 4. The distribution characteristics of all test ligands were generally comparable, with

the exception of the two compounds, which were anticipated to enter the BBB and CNS more easily, respectively.

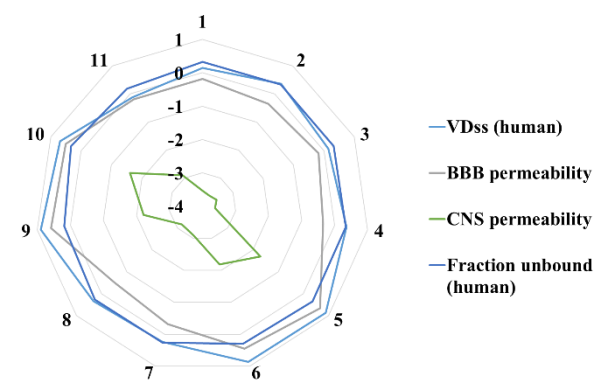


Figure 4. Prediction of test ligand distribution parameters with pkCSM. The test ligand predicted to have been the easiest to penetrate BBB and CNS was compounds 8 and 4, respectively.

The results of using SwissADME to measure metabolism parameters show that most test ligands (7 of 11) did not interact to inhibit several types of cytochromes, except compounds 5 (berberine), 6 (columbamine), 9, and 10 (palmatine), which could inhibit 2-3 types of cytochromes P450 isoform, as presented in Figure 5. The types of isoform include cytochrome P450 1A2 (CYP1A2), 2D6 (CYP2D6), and 3A4 (CYP3A4). Three ligands can simultaneously inhibit compounds 5, 6, and 9. Meanwhile, other compounds have practically low potential to become cytochrome P450 inhibitors.



Figure 5. Prediction of test ligand metabolism parameters with SwissADME. Compounds 5, 6, and 9 had the most chance as a cytochrome P450 inhibitor among other test ligands against three types of cytochrome P450 isoform: CYP1A2, CYP2D6, and CYP3A4.

Just one parameter was noted for excretion parameters: the total clearance from pkCSM, as Figure 6 illustrates. There was a significant difference in the total clearance value, in which compound 8 only had a total clearance of 0.468 log mL/min/kg, slightly smaller than compound 2 with 0.487 log mL/min/kg. In contrast, there are four compounds with a total clearance value above 1.2 log mL/min/kg: compounds 5, 6, 9, and 10. Among the four, the highest total clearance value is indicated by compound 5 with 1.278 log mL/min/kg.

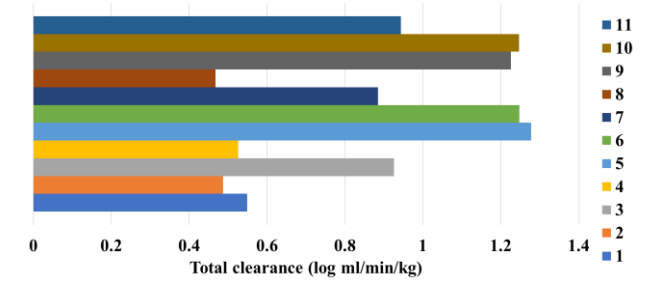


Figure 6. Prediction of test ligand excretion parameters with pkCSM. Compound 8 had the lowest total clearance with 0.468 log mL/min/kg, while the ligand with the highest total clearance was compound 5 with 1.278 log mL/min/kg.

Lastly, as seen in Figure 7, the predicted LD₅₀ values and the toxicity parameters were estimated using ProTox-II and toxicology model parameters for various target types and their probabilities. The first exciting thing was that each compound had at least a reasonably high probability (\geq 0.7) against one model: immunotoxicity. There were only two compounds with a probability of immunotoxicity of 0.7: compounds 7 (fibleucin) and 8, the lowest compared to other compounds. In addition, compounds 5, 6, 9, and 10 also had probabilities in the range of 0.73-0.87 to another toxicity model: mitochondrial membrane potential (sr_mmp). Compound 5 was the only one with a probability of the cytotoxicity (cyto) and aryl hydrocarbon receptor (nr_ahr) model, with a probability of 0.96 and 0.87, respectively. The predicted LD₅₀ values for all compounds were not too wide, between 200 and 555 mg/kg. There were four compounds with the lowest LD₅₀ values: compounds 5, 6, 9, and 10, and all four belong to predicted toxicity class III, which was toxic if swallowed.

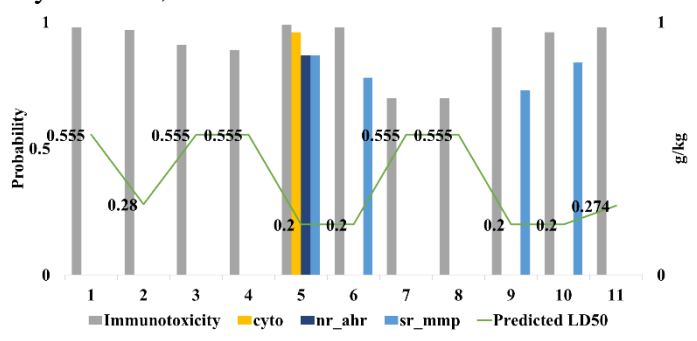


Figure 7. Prediction of test ligand toxicity parameters with ProTox-II. Compounds 7 and 8 show a moderate predicted value of LD₅₀ (555 mg/kg) with the lowest probability (0.7) to the immunotoxicity model. Compounds 5, 6, 9, and 10 show the lowest predicted value of LD₅₀ with 200 mg/kg, while compound 5 shows a high probability of the toxicity model with the highest number (four targets).

Despite its potential, research on *A. flava* needs to be more reported. One of the reasons is the toxic nature of some of its metabolites [39], which was confirmed in the results of this study. In Indonesia, using plant parts is explicitly prohibited for traditional medicine and health supplements [40]. However, research on its active metabolites is still being reported, especially for various infectious diseases [41], as reported by Maryani *et al.* [42]. Apart from not all of its toxic metabolites, some have high potential as antivirals, as summarized by Feng [43]. Therefore, developing this plant, especially for the SARS-CoV-2 M^{Pro} inhibitor, becomes rational, considering that there is very little data related to the following plants to deal with viral infections.

In silico studies of the metabolites of A. flava have not been widely reported, particularly concerning their potential as an antiviral. For example, research by Levita et al. [44] reported berberine as one of the metabolites of A. flava with the best docking results as inducible nitric oxide synthase inhibitors with ΔG of -7.9 kcal/mol, which was later corroborated by reports from Kolina et al. [45] on similar receptors. In that study, fibraurin showed one of the least favorable docking results with an ΔG of -4.4 kcal/mol. Our previous study also reported potential anticancer metabolites of A. flava through inhibiting Src kinase, which reported berberine as the best metabolite with ΔG -9.0 kcal/mol [46]. Meanwhile, the in silico study of A. flava, as our study first reported an antiviral as a neuraminidase inhibitor, reported fibleucin as the metabolite with the lowest ΔG at -8.12 kcal/mol [47]. Apart from that, practically no other studies have reported the potential of A. flava as an antiviral with an in silico approach, so the results of this study will provide an excellent update on the development

of A. flava, mainly because this study also reported predictive properties of ADMET, which had not been previously reported.

Two of the eleven metabolites studied stood out the most for different reasons: 6-hydroxyfibraurin and berberine. If 6-hydroxyfibraurin stands out in its potential affinity, berberine has an advantage in the similarity of its interactions. However, there are several reasons why, between the two compounds, 6-hydroxyfibraurin has more potency, especially when considering its ADMET properties. 6-hydroxyfibraurin tends to be less soluble in water but penetrates the BBB and CNS more easily than berberine. On the other hand, berberine can inhibit cytochrome P450, whereas 6-hydroxyfibraurin does not. The total clearance of berberine is more than two-fold greater than that of 6-hydroxyfibraurin. However, berberine has a higher probability of multiple toxicity models, with an LD₅₀ nearly three times that of 6-hydroxyfibraurin. Thus, it can be assumed that the toxicity potential of 6-hydroxyfibraurin is lower than that of berberine, which is confirmed by several studies reporting the toxicity of berberine [48-50]. On the other hand, no information on the toxicity of 6-hydroxyfibraurin or fibraurin as its non-hydrolyzed form has been reported.

The limitation of this study is the small number of test ligands. One of the reasons is that the reported number of metabolites from the stem of *A. flava* is still low, as the most widely used plant part empirically [51]. The results of the review by Cheng *et al.* showed the presence of several other compounds, which were also reported to be present in *A. flava* [32]. However, the part of the plant from which the compound was obtained needed to be explained. This research can also be continued with molecular dynamics studies to determine the stability of the interactions shown for each compound. Subsequently, direct *in vitro* studies with SARS-CoV-2 M^{Pro} and *in vivo* tests with test animal models need to be carried out to prove the validity and linearity of the results of the *in silico* studies that have been carried out.

4. Conclusions

In summary, of all the test ligands from *A. flava*, 6-hydroxyfibraurin showed the best potential as a SARS-CoV-2 M^{Pro} inhibitor. These compounds also exhibit varying properties of ADME that are still possible to develop and have the lowest relative toxicity. To demonstrate the potential and precise mechanism of these compounds as SARS-CoV-2 M^{Pro} inhibitors, additional *in vitro* and *in vivo* investigations are necessary.

Funding

The researchers are grateful to the Ministry of Research, Technology and Higher Education of the Republic of Indonesia for funding this research under Grant *Penelitian Dosen Pemula* with grant number 3/E/KPT/2018. All researchers have an equal contribution to this research and have agreed to the entire contents of this manuscript

Acknowledgments

The authors would like to thank Dr. Arthur E. Schneider from the Airlangga Writing Consultation Program, Universitas Airlangga, Indonesia, for helping improve the manuscript's readability.

Conflicts of Interest

The authors declare no conflict of interest. The funders had no role in the study's design; in the collection, analyses, or interpretation of data, in the writing of the manuscript, or in the decision to publish the results.

References

- 1. Wang, C.; Wang, Z.; Wang, G.; Lau, J.Y.-N.; Zhang, K.; Li, W. COVID-19 in early 2021: current status and looking forward. *Signal Transduct. Target. Ther.* **2021**, *6*, 114, https://doi.org/10.1038/s41392-021-00527-1.
- Pan, Y.; Zhang, L.; Yan, Z.; Lwin, M.O.; Skibniewski, M.J. Discovering optimal strategies for mitigating COVID-19 spread using machine learning: Experience from Asia. *Sustain. Cities Soc.* 2021, 75, 103254, https://doi.org/10.1016/j.scs.2021.103254.
- 3. Lindstrand, A.; Cherian, T.; Chang-Blanc, D.; Feikin, D.; O'Brien, K.L. The World of Immunization: Achievements, Challenges, and Strategic Vision for the Next Decade. *J. Infect. Dis.* **2021**, 224, S452-S467, https://doi.org/10.1093/infdis/jiab284.
- 4. Alsobaie, S. Understanding the Molecular Biology of SARS-CoV-2 and the COVID-19 Pandemic: A Review. *Infect. Drug Resist.* **2021**, *14*, 2259-2268, https://doi.org/10.2147/idr.s306441.
- 5. Tareq, A.M.; Emran, T.B.; Dhama, K.; Dhawan, M.; Tallei, T.E. Impact of SARS-CoV-2 delta variant (B.1.617.2) in surging second wave of COVID-19 and efficacy of vaccines in tackling the ongoing pandemic. *Hum. Vaccin. Immunother.* **2021**, *17*, 4126-4127, https://doi.org/10.1080/21645515.2021.1963601.
- El-Elimat, T.; AbuAlSamen, M.M.; Almomani, B.A.; Al-Sawalha, N.A.; Alali, F.Q. Acceptance and attitudes toward COVID-19 vaccines: A cross-sectional study from Jordan. *PLoS One* 2021, 16, e0250555, https://doi.org/10.1371/journal.pone.0250555.
- 7. Richman, D.D. COVID-19 vaccines: implementation, limitations and opportunities. *Glob. Health Med.* **2021**, *3*, 1-5, https://doi.org/10.35772/ghm.2021.01010.
- 8. Wu, C.; Liu, Y.; Yang, Y.; Zhang, P.; Zhong, W.; Wang, Y.; Wang, Q.; Xu, Y.; Li, M.; Li, X.; Zheng, M.; Chen, L.; Li, H. Analysis of therapeutic targets for SARS-CoV-2 and discovery of potential drugs by computational methods. *Acta Pharm. Sin. B* **2020**, *10*, 766-788, https://doi.org/10.1016/j.apsb.2020.02.008.
- Jin, Z.; Du, X.; Xu, Y.; Deng, Y.; Liu, M.; Zhao, Y.; Zhang, B.; Li, X.; Zhang, L.; Peng, C.; Duan, Y.; Yu, J.; Wang, L.; Yang, K.; Liu, F.; Jiang, R.; Yang, X.; You, T.; Liu, X.; Yang, X.; Bai, F.; Liu, H.; Liu, X.; Guddat, L.W.; Xu, W.; Xiao, G.; Qin, C.; Shi, Z.; Jiang, H.; Rao, Z.; Yang, H. Structure of M^{pro} from SARS-CoV-2 and discovery of its inhibitors. *Nature* 2020, 582, 289-293, https://doi.org/10.1038/s41586-020-2223-v.
- Hasan, A.H.; Hussen, N.H.; Shakya, S.; Jamalis, J.; Pratama, M.R.F.; Chander, S.; Kharkwal, H.; Murugesan, S. In silico discovery of multi-targeting inhibitors for the COVID-19 treatment by molecular docking, molecular dynamics simulation studies, and ADMET predictions. *Struct. Chem.* 2022, *33*, 1645-1665, https://doi.org/10.1007/s11224-022-01996-y.
- 11. Eastman, R.T.; Roth, J.S.; Brimacombe, K.R.; Simeonov, A.; Shen, M.; Patnaik, S.; Hall, M.D. Remdesivir: A Review of Its Discovery and Development Leading to Emergency Use Authorization for Treatment of COVID-19. *ACS Cent. Sci.* **2020**, *6*, 672-683, https://doi.org/10.1021/acscentsci.0c00489.
- 12. Tejera, E.; Munteanu, C.R.; López-Cortés, A.; Cabrera-Andrade, A.; Pérez-Castillo, Y. Drugs Repurposing Using QSAR, Docking and Molecular Dynamics for Possible Inhibitors of the SARS-CoV-2 M^{pro} Protease. *Molecules* **2022**, *25*, 5172, https://doi.org/10.3390/molecules25215172.
- 13. Yang, J.; Lin, X.; Xing, N.; Zhang, Z.; Zhang, H.; Wu, H.; Xue, W. Structure-Based Discovery of Novel Nonpeptide Inhibitors Targeting SARS-CoV-2 M^{pro}. *J. Chem. Inf. Model.* **2021**, *61*, 3917-3926, https://doi.org/10.1021/acs.jcim.1c00355.
- 14. Pratama, M.R.F.; Poerwono, H.; Siswodihardjo, S. Molecular Docking of Novel 5-O-benzoylpinostrobin Derivatives as SARS-CoV-2 Main Protease Inhibitors. *Pharm. Sci.* **2020**, *26*, S63-S77, https://doi.org/10.34172/PS.2020.57.
- 15. Salih, R.H.H.; Hasan, A.H.; Hussein, A.J.; Samad, M.K.; Shakya, S.; Jamalis, J.; Hawaiz, F.E.; Pratama, M.R.F. One-pot synthesis, molecular docking, ADMET, and DFT studies of novel pyrazolines as promising SARS-CoV-2 main protease inhibitors. *Res. Chem. Intermed.* **2022**, *48*, 4729-4751, https://doi.org/10.1007/s11164-022-04831-5.

- 16. Kumar Verma, A.; Kumar, V.; Singh, S.; Goswami, B.C.; Camps, I.; Sekar, A.; Yoon, S.; Lee, K.W. Repurposing potential of Ayurvedic medicinal plants derived active principles against SARS-CoV-2 associated target proteins revealed by molecular docking, molecular dynamics and MM-PBSA studies. *Biomed. Pharmacother.* **2021**, *137*, 111356, https://doi.org/10.1016/j.biopha.2021.111356.
- 17. Bharadwaj, S.; Dubey, A.; Yadava, U.; Mishra, S.K.; Kang, S.G.; Dwivedi, V.D. Exploration of natural compounds with anti-SARS-CoV-2 activity via inhibition of SARS-CoV-2 M^{pro}. *Brief. Bioinform.* **2021**, 22, 1361-1377, https://doi.org/10.1093/bib/bbaa382.
- 18. Gupta, S.; Singh, A.K.; Kushwaha, P.P.; Prajapati, K.S.; Shuaib, M.; Senapati, S.; Kumar, S. Identification of potential natural inhibitors of SARS-CoV2 main protease by molecular docking and simulation studies. *Biomol. Struct. Dyn.* **2021**, *39*, 4334-4345, https://doi.org/10.1080/07391102.2020.1776157.
- 19. Enmozhi, S.K.; Raja, K.; Sebastine, I.; Joseph, J. Andrographolide as a potential inhibitor of SARS-CoV-2 main protease: an in silico approach. *J. Biomol. Struct. Dyn.* **2021**, *39*, 3092-3098, https://doi.org/10.1080/07391102.2020.1760136.
- Ahmad, S.; Abbasi, H.W.; Shahid, S.; Gul, S.; Abbasi, S.W. Molecular docking, simulation and MM-PBSA studies of *nigella sativa* compounds: a computational quest to identify potential natural antiviral for COVID-19 treatment. *J. Biomol. Struct. Dyn.* 2021, 39, 4225-4233, https://doi.org/10.1080/07391102.2020.1775129.
- van de Sand, L.; Bormann, M.; Alt, M.; Schipper, L.; Heilingloh, C.S.; Steinmann, E.; Todt, D.; Dittmer, U.; Elsner, C.; Witzke, O.; Krawczyk, A. Glycyrrhizin Effectively Inhibits SARS-CoV-2 Replication by Inhibiting the Viral Main Protease. *Viruses* 2021, 13, 609, https://doi.org/10.3390/v13040609.
- 22. Ghosh, A.; Chakraborty, M.; Chandra, A.; Alam, M.P. Structure-activity relationship (SAR) and molecular dynamics study of withaferin-A fragment derivatives as potential therapeutic lead against main protease (M^{pro}) of SARS-CoV-2. *J. Mol. Model.* **2021**, *27*, 97, https://doi.org/10.1007/s00894-021-04703-6.
- 23. de Oliveira, V.M.; da Rocha, M.N.; Magalhães, E.P.; da Silva Mendes, F.R.; Marinho, M.M.; de Menezes, R.R.P.P.B.; Sampaio, T.L.; dos Santos, H.S.; Martins, A.M.C.; Marinho, E.S. Computational approach towards the design of artemisinin–thymoquinone hybrids against main protease of SARS-COV-2. *Futur. J. Pharm. Sci.* **2021**, *7*, 185, https://doi.org/10.1186/s43094-021-00334-z.
- 24. Ghosh, R.; Chakraborty, A.; Biswas, A.; Chowdhuri, S. Evaluation of green tea polyphenols as novel corona virus (SARS CoV-2) main protease (Mpro) inhibitors an *in silico* docking and molecular dynamics simulation study. *J. Biomol. Struct. Dyn.* **2021**, *39*, 4362-4374, https://doi.org/10.1080/07391102.2020.1779818.
- 25. Ansori, A.N.M.; Kharisma, V.D.; Parikesit, A.A.; Dian, F.A.; Probojati, R.T.; Rebezov, M.; Scherbakov, P.; Burkov, P.; Zhdanova, G.; Mikhalev, A. Bioactive Compounds from Mangosteen (Garcinia mangostana L.) as an Antiviral Agent via Dual Inhibitor Mechanism against SARSCoV- 2: An In Silico Approach. *Pharmacogn. J.* **2022**, *14*, 85-90, http://dx.doi.org/10.5530/pj.2022.14.12.
- 26. Khanna, K.; Kohli, S.K.; Kaur, R.; Bhardwaj, A.; Bhardwaj, V.; Ohri, P.; Sharma, A.; Ahmad, A.; Bhardwaj, R.; Ahmad, P. Herbal immune-boosters: Substantial warriors of pandemic Covid-19 battle. *Phytomedicine* **2021**, *85*, 153361, https://doi.org/10.1016/j.phymed.2020.153361.
- 27. Pratama, M.R.F.; Suratno, S.; Mulyani, E. ANTIBACTERIAL ACTIVITY OF AKAR KUNING (ARCANGELISIA FLAVA) SECONDARY METABOLITES: MOLECULAR DOCKING APPROACH. *Asian J. Pharm. Clin. Res.* **2018**, *11*, 447-451, http://dx.doi.org/10.22159/ajpcr.2018.v11i11.29189.
- 28. Suzuki, T.; Kiyotani, T.; Maeda, M.; Katayama, T.; Tomita-Yokotani, K.; Syafii, W.; Muladi, S. Furanoditerpenes from *Arcangelisia flava* (L.) Merr. and their antifungal activity. *Phytochem. Lett.* **2011**, *4*, 333-336, https://doi.org/10.1016/j.phytol.2011.07.002.
- 29. Och, A.; Podgórski, R.; Nowak, R. Biological Activity of Berberine—A Summary Update. *Toxins* **2020**, *12*, 713, https://doi.org/10.3390/toxins12110713.
- 30. Hori, T.; Kiang, A.K.; Nakanishi, K.; Sasaki, S.; Woods, M.C. The structures of fibraurin and a minor product from *fibraurea chloroleuca*. *Tetrahedron* **1967**, 23, 2649-2656, https://doi.org/10.1016/0040-4020(67)85129-9.
- 31. Pratama, M.R.F.; Praditapuspa, E.N.; Kesuma, D.; Poerwono, H.; Widiandani, T.; Siswodihardjo, S. *Boesenbergia Pandurata* as an Anti-Breast Cancer Agent: Molecular Docking and ADMET Study. *Lett. Drug Des. Discov.* **2022**, *19*, 606-626, https://doi.org/10.2174/1570180819666211220111245.
- 32. Cheng, Q.; Li, F.; Yan, X.; He, J.; Zhang, H.; Wang, C.; He, Y.; Li, Z. Phytochemical and pharmacological studies on the genus *Arcangelisia*: A mini review. *Arab. J. Chem.* **2021**, *14*, 103346, https://doi.org/10.1016/j.arabjc.2021.103346.

- 33. Nguyen, H.L.; Thai, N.Q.; Truong, D.T.; Li, M.S. Remdesivir Strongly Binds to Both RNA-Dependent RNA Polymerase and Main Protease of SARS-CoV-2: Evidence from Molecular Simulations. *J. Phys. Chem. B* **2020**, *124*, 11337-11348, https://doi.org/10.1021/acs.jpcb.0c07312.
- 34. Mahal, A.; Al-Janabi, M.; Eyüpoğlu, V.; Alkhouri, A.; Chtita, S.; Kadhim, M.M.; Obaidullah, A.J.; Alotaibi, J.M.; Wei, X.; Pratama, M.R.F. Molecular docking, drug-likeness and DFT study of some modified tetrahydrocurcumins as potential anticancer agents. *Saudi Pharm. J.* **2024**, *32*, 101889, https://doi.org/10.1016/j.jsps.2023.101889.
- 35. Pratama, M.R.F.; Poerwono, H.; Siswodihardjo, S. Introducing a two-dimensional graph of docking score difference vs. similarity of ligand-receptor interactions. *Indones J. Biotechnol.* **2021**, 26, 54-60, https://doi.org/10.22146/ijbiotech.62194.
- 36. Pratama, M.R.F.; Poerwono, H.; Siswodihardjo, S. ADMET properties of novel 5-*O*-benzoylpinostrobin derivatives. *J. Basic Clin. Physiol. Pharmacol.* **2019**, *30*, 20190251, https://doi.org/10.1515/jbcpp-2019-0251.
- 37. Sukardiman; Ervina, M.; Fadhil Pratama, M.R.; Poerwono, H.; Siswodihardjo, S. The coronavirus disease 2019 main protease inhibitor from *Andrographis paniculata* (Burm. f) Ness. *J. Adv. Pharm. Technol. Res.* **2020**, *11*, 157-162, https://doi.org/10.4103/japtr.japtr_84_20.
- 38. Souza, S.A.; Held, A.; Lu, W.J.; Drouhard, B.; Avila, B.; Leyva-Montes, R.; Hu, M.; Miller, B.R.; Ng, H.L. Mechanisms of allosteric and mixed mode aromatase inhibitors. *RSC Chem. Biol.* **2021**, 2, 892-905, https://doi.org/10.1039/D1CB00046B.
- 39. Pramono, S.; Paramawidhita, R.Y.T.; Marini, M.; Bachri, M.S. Comparative Effects of Yellow Root (Arcangelisia flava (L.) Merr.) Decoctions with Water and Brackish Water on Kidneys and Uterus in Wistar Rats. *Trad. Med. J.* **2020**, *25*, 118-122, https://doi.org/10.22146/mot.55178.
- 40. Dianasari, W.; Nadjib, M. SUPERVISION OF TRADITIONAL MEDICINES CONTAINING UNDECLARED SUBSTANCE: ANALYSIS OF INDONESIAN FDA MONITORING DATA FOR 2012 2021. *J. Indones. Health Policy Adm.* **2022**, *7*, 196-205, http://dx.doi.org/10.7454/ihpa.v7i1.5858.
- 41. Ramadani, A.P.; Paloque, L.; Belda, H.; Tamhid, H.A.; Masriani; Jumina; Augereau, J.-M.; Valentin, A.; Wijayanti, M.A.; Mustofa; Benoit-Vical, F. Antiprotozoal properties of Indonesian medicinal plant extracts. *J. Herb. Med.* **2018**, *11*, 46-52, https://doi.org/10.1016/j.hermed.2017.06.004.
- 42. Maryani; Rosita; Monalisa, S.S.; Rozik, M. In vitro test of natural antibacterial activity of yellow-fruit moonseed Arcangelisia flava Merr. Leaf on bacterium Pseudomonas fluorescens under different doses. *AACL Bioflux* **2018**, *11*, 288-294.
- 43. Feng, J.Y. Addressing the selectivity and toxicity of antiviral nucleosides. *Antivir. Chem. Chemother.* **2018**, *26*, 2040206618758524, https://doi.org/10.1177/2040206618758524.
- 44. Jutti Levita, R.P.; , J.K., Tiana Milanda, Mutakin Mutakin, Irma Melyani Puspitasari, Nyi Mekar Saptarini, Sri Adi Sumiwi. Pharmacophore modeling and molecular docking of phytoconstituents in Morus sp. and Arcangelisia flava against nitric oxide synthase for antiinflammatory discovery. *J. Appl. Pharm. Sci.* **2018**, 8, 53-59, http://dx.doi.org/10.7324/JAPS.2018.81207.
- 45. Kolina, J.; Sumiwi, S.A.; Levita, J. MODE IKATAN METABOLIT SEKUNDER DI TANAMAN AKAR KUNING (Arcangelisia flava L.) DENGAN NITRAT OKSIDA SINTASE. *Fitofarmaka J. Ilmiah Farmasi* **2018**, *8*, 45-52, https://doi.org/10.33751/jf.v8i1.1171.
- 46. Pratama, M.R.F.; Mulyani, E.; Suratno, S. Molecular Docking Study of Akar Kuning (Arcangelisia flava) Secondary Metabolites as Src Inhibitor. *Indones. J. Cancer Chemopreven.* **2019**, *10*, 122-130, http://dx.doi.org/10.14499/indonesianjcanchemoprev10iss3pp122-130.
- 47. Pratama, M.R.F. Akar Kuning (Arcangelisia Flava) As Neuraminidase Inhibitor: Molecular Docking And Pharmacophore Optimization Approach. In Proceedings of the 2nd Sari Mulia International Conference on Health and Sciences 2017 (SMICHS 2017), Banjarmasin, Indonesia, 8-9 December 2017; Mahdiyah, D., Nurdin, F., Fajriannoor, M., Sari, P.V.D., Al Kahfi, R., Amelia, R., Iswandari, N.D., Dona, S., ; Eds.; Atlantis Press: Paris, France, 2017; 502-511, https://doi.org/10.2991/smichs-17.2017.63.
- 48. Martini, D.; Pucci, C.; Gabellini, C.; Pellegrino, M.; Andreazzoli, M. Exposure to the natural alkaloid Berberine affects cardiovascular system morphogenesis and functionality during zebrafish development. *Sci. Rep.* **2020**, *10*, 17358, https://doi.org/10.1038/s41598-020-73661-5.
- 49. Zhang, M.Y.; Yu, Y.Y.; Wang, S.F.; Zhang, Q.; Wu, H.W.; Wei, J.Y.; Yang, W.; Li, S.Y.; Yang, H.J. Cardiotoxicity evaluation of nine alkaloids from *Rhizoma Coptis. Hum. Exp. Toxicol.* **2018**, *37*, 185-195, https://doi.org/10.1177/0960327117695633.

- 50. Feng, P.; Zhao, L.; Guo, F.; Zhang, B.; Fang, L.; Zhan, G.; Xu, X.; Fang, Q.; Liang, Z.; Li, B. The enhancement of cardiotoxicity that results from inhibiton of CYP 3A4 activity and hERG channel by berberine in combination with statins. *Chem. Biol. Interact.* **2018**, 293, 115-123, https://doi.org/10.1016/j.cbi.2018.07.022.
- 51. Wardah; Sundari, S. Ethnobotany study of Dayak society medicinal plants utilization in Uut Murung District, Murung Raya Regency, Central Kalimantan. *IOP Conf. Ser.: Earth Environ. Sci.* **2019**, 298, 012005, https://dx.doi.org/10.1088/1755-1315/298/1/012005.